Europace (2011) **13**, 1494–1500
doi:10.1093/europace/eur168

Spatiotemporal electrophysiological changes in a murine ablation model

Scott A. Bernstein, Srikant Duggirala, Michael Floberg, Pehr Elfvendal, Laura M. Kuznekoff, Joshua M. Lader, Carolina Vasquez, and Gregory E. Morley*

The Leon H. Charney Division of Cardiology, New York University School of Medicine, 522 First Avenue, 8th Floor, Smilow Building, New York, NY 10016, USA

Received 31 January 2011; accepted after revision 6 May 2011; online publish-ahead-of-print 28 June 2011

Aims High recurrence rates after complex radiofrequency ablation procedures, such as for atrial fibrillation, remain a major clinical problem. Local electrophysiological changes that occur following cardiac ablation therapy are incompletely described in the literature. The purpose of this study was to determine whether alterations in conduction velocity, action potential duration (APD), and effective refractory period resolve dynamically following cardiac ablation.

Methods and results Lesions were delivered to the right ventricle of mice using a subxiphoid approach. The sham-operated control group (SHAM) received the same procedure without energy delivery. Hearts were isolated at 0, 1, 7, 30, and 60 days following the procedure and electrophysiological parameters were obtained using high-resolution optical mapping with a voltage-sensitive dye. Conduction velocity was significantly decreased at the lesion border in the 0, 7, and 30 day groups compared to SHAM. APD_{70} at the lesion border was significantly increased at all time points compared to SHAM. Effective refractory period was significantly increased at the lesion border at 0, 1, 7, and 30 days but not at 60 days post-ablation. This study demonstrated that post-ablation electrophysiological changes take place immediately following energy delivery and resolve within 60 days.

Conclusions Cardiac ablation causes significant electrophysiological changes both within the lesion and beyond the border zone. Late recovery of electrical conduction in individual lesions is consistent with clinical data demonstrating that arrhythmia recurrence is associated with failure to maintain bi-directional conduction block.

Keywords Ablation • Conduction block • Murine model

Introduction

Catheter-based ablation is currently the most effective procedure performed in patients with a variety of atrial and ventricular arrhythmias. Complex arrhythmias, such as atrial fibrillation (AF) and ventricular tachycardia, often require extensive lesion sets to achieve acute success.[1–8] Recurrence rates of these arrhythmias are higher and extensive lesions sets are often pro-arrhythmic.[9] Approximately 25–50% of patients with persistent AF will need a repeat procedure within 1 year.[10,11] High recurrence rates are attributed to a failure to maintain bi-directional conduction block across linear sets and reconnection of pulmonary veins.

Lesion healing after cardiac ablation therapy is a highly dynamic process that induces complex changes in structure and local electrophysiological properties. Relatively few studies have examined the acute and chronic electrophysiological changes that occur following cardiac ablation. Studies in rabbit hearts during and immediately after application of energy have suggested that cardiac ablation results in significant decreases in effective refractory period (ERP) and action potential duration (APD) in the region surrounding the lesion.[12,13] These parameters returned to baseline values within minutes following energy application. However, a major limitation of these studies is that they were performed in isolated perfused hearts, which could have an effect on the biophysics of energy delivery. In addition, the electrophysiological consequences of ablation may differ in the absence of an acute inflammatory response. Short-term studies where ablation therapy was applied *in vivo* have suggested electrophysiological parameters in the region surrounding the lesion return to baseline values within 1–3 weeks.[13] To date, there has been no study

* Corresponding author. Tel: +1 212 263 4130; fax: +1 212 263 4129, Email: Gregory.Morley@nyumc.org

systematic evaluation of the dynamic spatiotemporal electrophysiological changes associated with sub-acute and chronic transmural lesions using an *in vivo* model of cardiac ablation.

Materials and methods

Mice

All studies were performed using female C57/BL6 wild-type mice aged 10 weeks ($n = 85$). All animal care protocols were approved and conformed to institutional and National Institutes of Health guidelines.

Ablation protocol

Mice were anaesthetized with inhaled 1.5% isoflurane, a subxiphoidal incision was made and the diaphragm was visualized. Using a micromanipulator, a stimulation probe (FHC Inc., Bowdoin, ME, USA) was inserted through the diaphragm to make contact with the right ventricular (RV) free wall near the apex (see *Figure 1A*). Pulsed direct current ablation energy was applied to induce a thermal injury. The following settings were used: 8.0 mA, 100 ms interval, 30 ms pulse duration for 90 s. After removal of the stimulation probe, the incision was closed with 7.5 mm wound clips and the animal was allowed to recover until extraction of the heart. Hearts were studied at five different time points: 0 ($n = 11$), 1 ($n = 15$), 7 ($n = 10$), 30 ($n = 12$), and 60 ($n = 11$) days following RV lesion delivery. Hearts for the Day 0 group were isolated immediately following the ablation procedure. For the sham-operated control group (SHAM), the same procedure was performed without delivery of energy.

Optical mapping

High-resolution optical mapping of perfused hearts was performed as previously described.[14] Briefly, mice were heparinized (30 I.U. IP) and euthanized with 100% CO_2 followed by cervical dislocation. Hearts were extracted through a median sternotomy, the aorta was cannulated, and the hearts were Langendorff perfused (1.0–2.0 mL/min) with 37°C oxygenated (95% O_2 5% CO_2) Tyrode's solution containing (in mM): $CaCl_2$ 1.8, $MgCl_2$ 1.0, KH_2PO_4 1.2, NaCl 130, KCl 4.7, $NaHCO_3$ 24, and glucose 11.1; albumin 0.052 g/L. Heart motion was limited with the excitation uncoupler, blebbistatin (5 μM).[15] After 10 min of perfusion, hearts were perfused with 20 μM di-4-ANNEPS (Invitrogen Corp., Carlsbad, CA, USA). Steady-state fluorescent levels were achieved within ~10 min. High-resolution optical mapping studies were performed on an upright microscope (MVX10, Olympus Inc., Brea, CA, USA) equipped with a high-speed complementary metal oxide semiconductor camera (MiCAM ULTIMA L, SciMedia Ltd, Costa Mesa, CA, USA). Hearts were excluded from the study if the epicardial lesion diameter was <1 mm at the time of explant.

Electrophysiological parameters

Hearts were paced on the epicardial surface using a platinum bipolar electrode connected to a signal generator (Pulsar 6i, FHC Inc., Bowdoin, ME, USA). Hearts were paced at a basic cycle length of 100 ms using 5 ms pulses at twice diastolic threshold. Electrograms (EGM) were recorded using a bipolar electrode at the lesion border, 4 mm, and >4 mm from the lesion centre during normal sinus rhythm. Electrograms were amplified, low-pass filtered (cut-off 250 Hz), and digitized (5 kHz) for off-line analysis (CyberAmp 380 signal conditioner and Digidata 1440A, Molecular Devices, Sunnyvale, CA, USA). Electrograms amplitudes at the lesion border and 4 mm were normalized to EGM amplitudes measured at >4 mm for each animal. Effective refractory period was determined by applying a train of 10 S_1 stimuli at 100 ms cycle length followed by a single S_2 pre-mature stimulus. The S_1–S_2 coupling interval was decreased by 2 ms from 100 ms until loss of ventricular capture. Effective refractory period was defined as the shortest S_1–S_2 coupling interval that induced a conducted response.

Data analysis

Conduction velocity (CV) and APD_{70} were determined offline using a custom software package as previously described.[16] Each electrophysiological parameter was calculated by averaging a 10 × 10 pixel area at the border, 4 mm from the lesion centre, and at distances >4 mm.

Histological analysis

Hearts were cut sagittally into 1 mm sections with a razor blade using a stainless-steel heart slicer (Zivic Instruments, Pittsburgh, PA, USA). Sections were fixed with 10% formaldehyde and stored at room temperature. Tissue was embedded in paraffin and cut into 5 μm sections. Sections were stained with either Gomori's trichrome or haematoxylin and eosin (H&E) according to the manufacturer's instructions and evaluated under a light microscope (Leica DM4000B). Images were captured with a digital camera. Fibrosis content was determined from cross sections of the lesion in a blinded fashion using Image-Pro Plus 5.0 software (Media Cybernetics, Bethesda, MD, USA). Fibrosis from two regions was quantified, the inferior border of the lesion and a remote area 4 mm from the lesion. Data were acquired from at least five sections per heart, which were analysed by quantifying blue pixel content as a percentage of the total tissue area.

Lesion quantification

Lesions were photographed with an upright microscope (SZX-12, Olympus Inc., Brea, CA, USA) and a digital camera. The lesion area was determined by approximating the cross-sectional area of each lesion as an ellipse, and using the formula $A = \pi ab$.

Statistical analysis

Statistical analysis was performed using the Excel software package. Group comparisons were performed using analysis of variance followed by the Student's *t*-test. All *P* values were calculated using two-tailed tests and $P < 0.05$ was considered significant.

Results

Gross evaluation of hearts showed that application of energy resulted in a well-demarcated area of injury. Cross-sections in the sagittal plane demonstrated the affected area extended through to the endocardial margin. Injury to ventricular septum was not observed in any hearts. *Figure 1B–D* show a representative

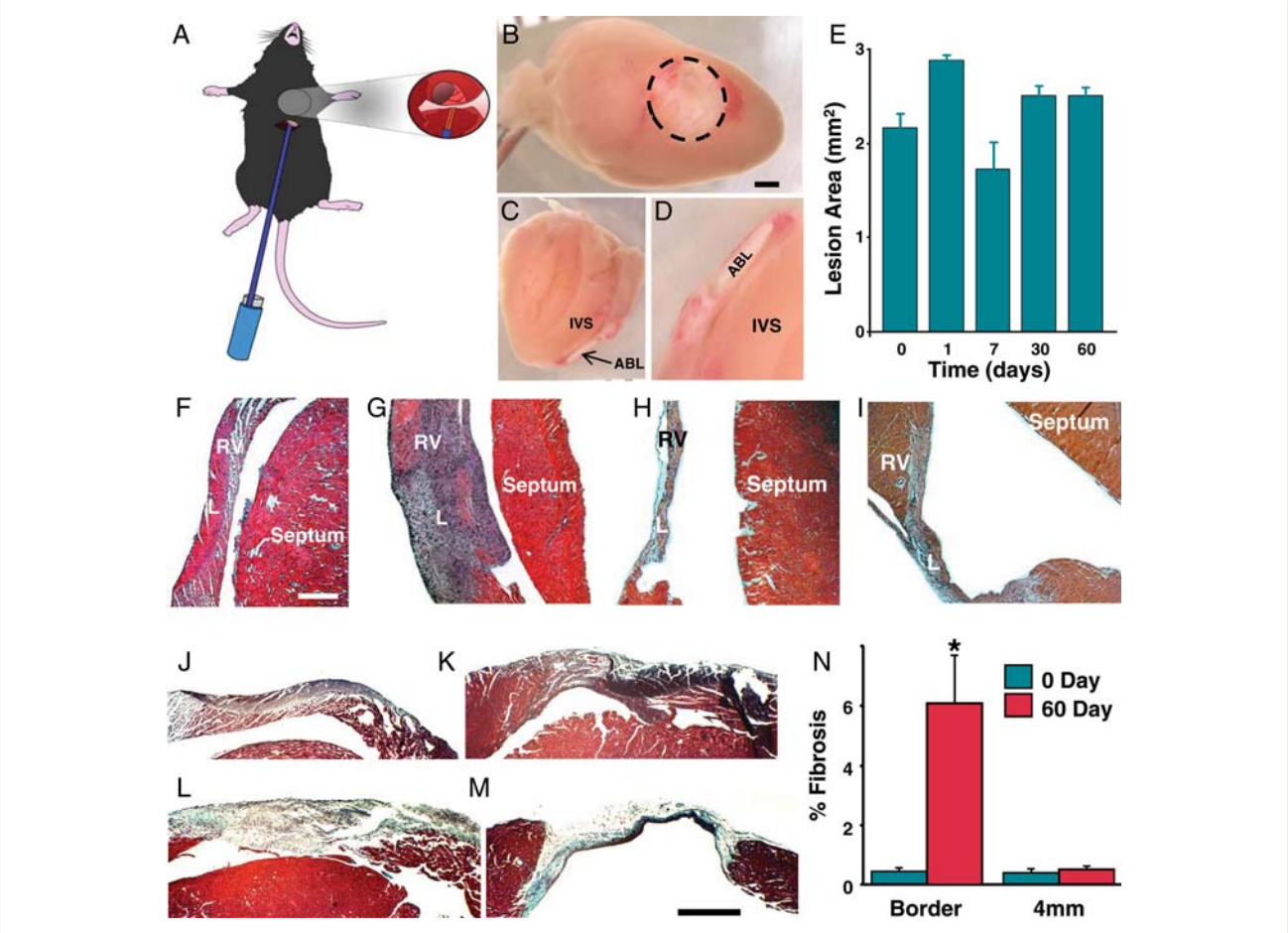

Figure 1 Cross views of lesion and histological analysis. (*A*) Diagram of mouse instrumented with ablation electrode. Inset shows the electrode in contact with the heart. (*B*) Cross view of right ventricular lesion 1 day after ablation. Dashed line indicates lesion border. Scale bar is 1 mm. (*C*) Sagittal cross-sectional image showing transmural lesion. Ablation lesion. Intervnricular septum. (*D*) Magnified view of (C). (*E*) Average lesion area at different times following ablation. (*F–I*) H&E stained sagittal cross section of lesions at 0, 7, 30, and 60 days after energy delivery, respectively. RV, right ventricle; L, lesion. Scale bar is 50 mm. (*J–M*) Representative Gomori's trichrome-stained sections 0, 1, 7, and 60 days after energy delivery, respectively. Bar = 0.5 mm. *N*, average per cent fibrosis values at 0 and 60 days after energy delivery ($n = 3$) for each group. Asterisk indicates $P = 0.03$ compared with border at 0 day.

lesion at Day 1 after application of energy. At the early time points (0, 1, and 7 days), there was a central core surrounded by a haemorrhagic zone. At the later time points (30 and 60 days) lesions appeared lighter without a distinct haemorrhagic border. Lesion area was not significantly different for any of the post-ablation time points (*Figure 1E*).

Histological analysis was performed on a subgroup of hearts ($n = 12$) to determine the transmural extent of the lesions and the presence of inflammatory changes. *Figure 1F–I* show representative H&E-stained sections at Day 0, 7, 30, and 60. At Days 0 and 1, there was evidence of irreversible myocardial injury characterized by disorganized cellular structure and basophilic stippling, with a poorly defined injury border zone. On Day 7, there is a demarcation between the injured and viable tissue. Consistent with previous studies, an influx of inflammatory cellular infiltrate occurred at this time point. Thirty days after energy delivery, there were signs of mature scar characterized by thinning of the affected area and a clearly demarcated border zone. The histological appearance of the scar did not change between 30 and 60 days after energy delivery. There were no gross or histological signs of injury in SHAM hearts (data not shown). *Figure 1J–N* show temporal and regional changes in fibrosis following energy delivery. Interstitial fibrosis was present at low levels and was not spatially related to the lesion at Days 0, 1, and 7. Sixty days after energy delivery, the lesion centre was characterized by wall thinning and extensive collagen deposition. In addition, interstitial fibrosis was present in the lesion border zone 60 days after energy delivery. Quantification of fibrosis at the lesion border showed a significant increase at 60 days compared with Day 0. Distal regions did not show changes in fibrosis.

Electrophysiological parameters

Local EGM amplitudes were measured to evaluate the electrophysiological extent of injury. *Figure 2A* and *B* show EGM

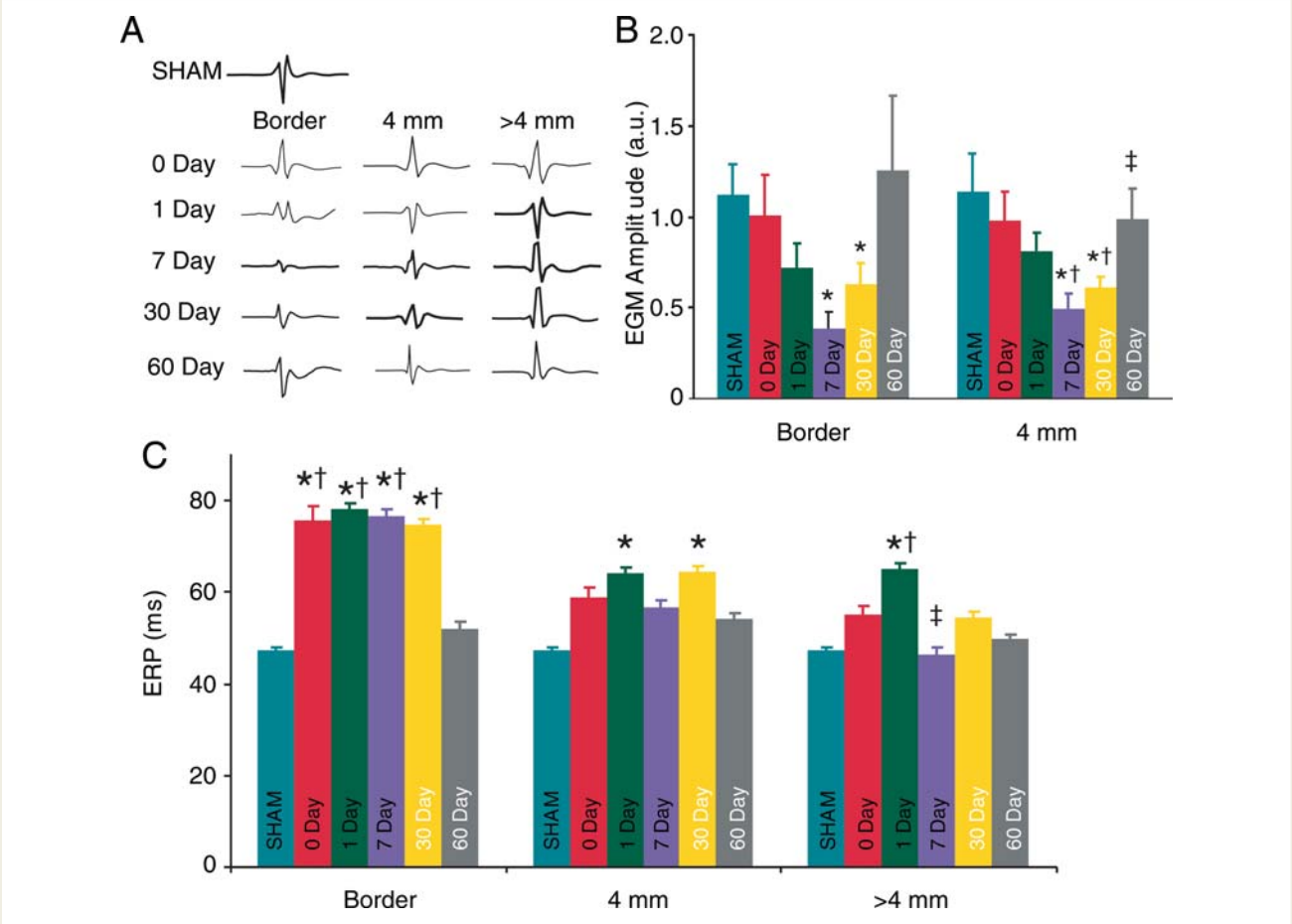

Figure 2 Spatial and temporal changes in local electrogram amplitudes and effective refractory period. (*A*) Examples of local electrogram traces. (*B*) Average electrograms amplitude. *, †, and ‡ indicate significant differences compared with SHAM, Days 0 and 7, respectively. (*C*) Average effective refractory period measured at the border, 4 and 6 mm from the lesion. Asterisk indicates significant differences compared with SHAM. Dagger and double dagger indicates significant differences compared with 60 and 1 day, respectively.

amplitudes at the lesion border and 4 mm away from the lesion were significantly decreased compared with SHAM (1.09 ± 0.17, $n = 10$) at post-ablation Day 7 (0.39 ± 0.09, $n = 7$, $P = 0.0006$ and 0.50 ± 0.08, $n = 7$, $P = 0.002$, respectively), and 30 (0.62 ± 0.12, $n = 10$, $P = 0.014$ and 0.61 ± 0.06, $n = 10$, $P = 0.002$ respectively). Sixty days post-ablation average EGM amplitude at the border and 4 mm away returned to baseline levels and were not significantly different from either the Day 0 or SHAM. Electrograms amplitudes measured at the lesion border did not change with time. Electrograms amplitudes 4 mm from the border were significantly decreased at Days 7 and 30 compared with Day 0. In addition, EGM amplitudes significantly increased between 7 and 60 days post-ablation.

Figure 2C shows average ERP values measured for all groups at the lesion border, 4 mm, and >4 mm from the lesion border. The effective refractory period was significantly increased at the lesion border from Day 0 to 30 compared with SHAM. At a distance of 4 mm from the lesion centre, average ERPs were significantly increased at 1 day and 30 days post-ablation compared with SHAM. At distances >4 mm from the lesion border, average ERP values were significantly increased only 1 day post-ablation. Average ERP values were not significantly different for any region measured 60 days post-ablation compared with SHAM. Effective refractory period values measured at the lesion border were significantly longer at 0 through Day 30 compared with Day 60.

Figure 3A–F show representative activation maps for SHAM and post-ablation Days 0, 1, 7, 30, and 60, respectively. Activation in the SHAM hearts was smooth and uniform throughout the RV surface. Activation maps from all ablated hearts showed a region that failed to activate surrounded by an area of regional conduction heterogeneity. *Figure 3G* shows average CV values measured for all groups at the lesion border, 4 mm, and >4 mm from the lesion border. Conduction velocity was significantly decreased at the lesion border at Day 0, 7, and 30 (0.36 ± 0.01 m/s, $P = 0.0000091$; 0.35 ± 0.01 m/s, $P = 0.000034$; 0.41 ± 0.01 m/s, $P = 0.004$, respectively) compared with SHAM (0.52 ± 0.01 m/s). Conduction velocity values were not significantly different at the lesion border at Day 1 (0.49 ± 0.01 m/s, $P = 0.64$) or Day 60 (0.54 ± 0.01 m/s, $P = 0.75$). Four millimetres from the lesion

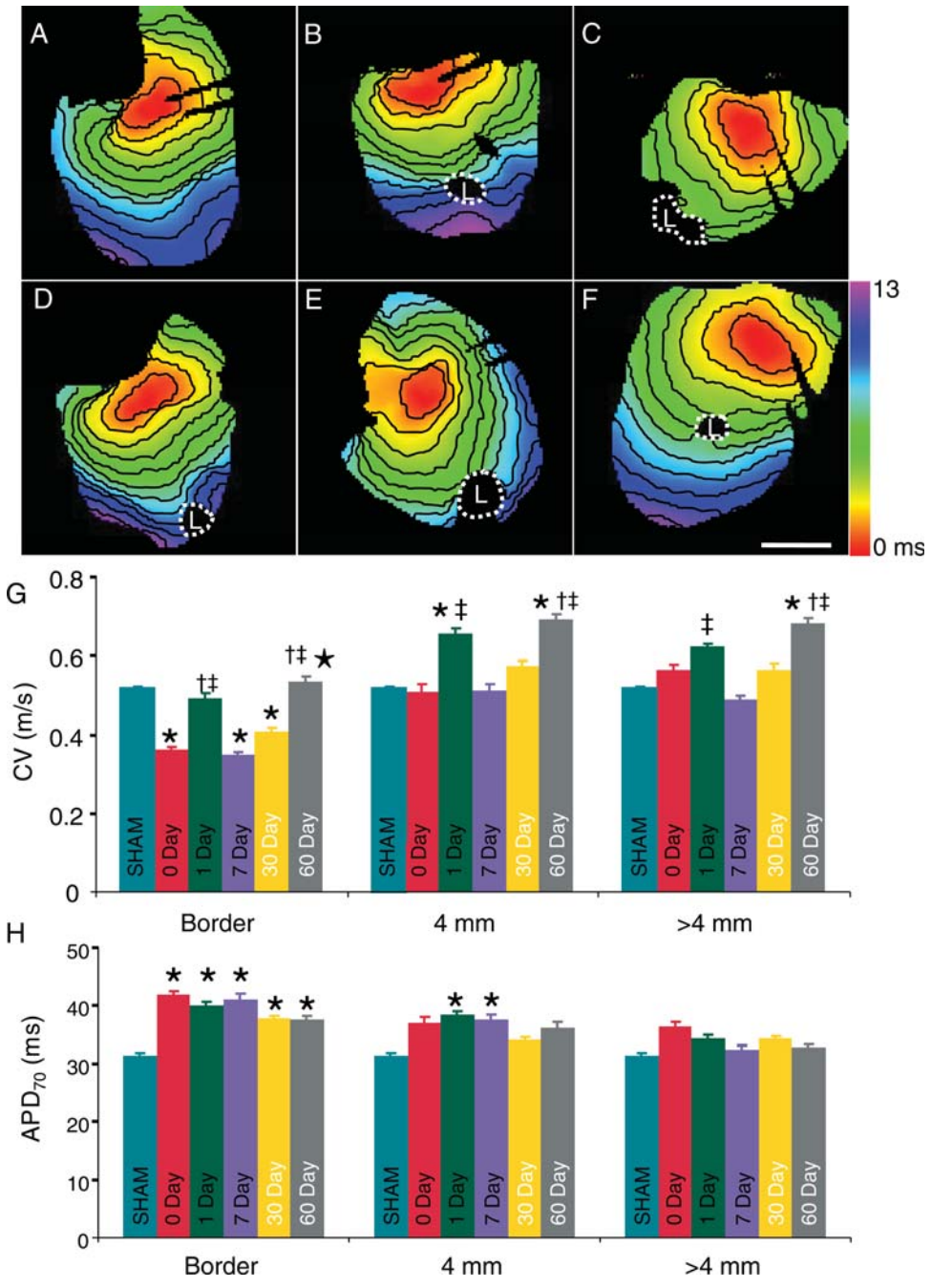

Figure 3 Spatial and temporal changes in conduction and APD_{70}. (*A–F*) Activation maps of right ventricular free wall recorded from SHAM, 0, 1, 7, 30, and 60 days after ablation, respectively. Lesions are outlined with white dashes. Scale bar is 2.5 mm; isochronal lines are spaced 1 ms apart. (*G*) Average CV measured at the border, 4 mm and >4 mm from the border of lesion. Asterisk indicates significant differences compared with SHAM. Dagger indicates significant differences compared with Day 0. Double dagger indicates significant differences compared with Day 7. Filled star indicates significant differences compared with Day 30. (*H*) Bar chart showing average APD_{70} values. Asterisk indicates significant differences compared with SHAM.

border CV values were also not significantly different at Days 0, 7, or 30. However, CV values were significantly faster compared with SHAM in the 1- and 60-day groups (0.66 ± 0.01 m/s, $P = 0.02$ and 0.69 ± 0.01 m/s, $P = 0.001$, respectively). Greater than 4 mm from the lesion, CV was significantly increased at Day 60 (0.68 ± 0.01 m/s, $P = 0.001$) compared with SHAM. At the lesion border, CV values at Days 1 and 60 were significantly increased compared with Days 0 and 7. In addition, Day 60 was significantly faster than Day 30. At 4 mm and >4 mm CV values at Day 60 were significantly faster compared with Day 0. Additionally, at

4 mm and >4 mm CV values at Days 1 and 60 were significantly increased compared with Day 7.

Figure 3H shows the spatial and temporal changes of APD_{70}. APD_{70} values were significantly longer at the border of the lesion at Day 0 (41.9 ± 0.68 ms, $P = 0.001$), Day 1 (40.0 ± 0.69 ms, $P = 0.02$), Day 7 (41.0 ± 1.07 ms, $P = 0.02$), Day 30 (37.9 ± 0.33 ms, $P = 0.001$), and Day 60 (37.6 ± 0.76 ms, $P = 0.048$) compared with SHAM (31.5 ± 0.37 ms). Additionally, APD_{70} was significantly longer at a greater distance from the lesion centre (4 mm) at Day 1 (38.4 ± 0.6 ms, $P = 0.036$) and Day 7 (37.7 ± 0.85 ms, $P = 0.049$) compared with SHAM. There were no significant differences in APD_{70} at 4 mm from the lesion centre at any of the other post-ablation times compared with SHAM. APD_{70} values were unchanged at distances >4 mm from the lesion at all time points. Action potential duration values in the ablated groups measured at the border, 4 mm or >4 mm did not significantly change with time after ablation.

Discussion

In this study we successfully developed a novel murine survival model of transmural ablation. We assessed the histological and electrophysiological changes over a large area and at multiple time points. Our data demonstrate that at the lesion border CV, APD, and ERP are all significantly altered following cardiac ablation. Action potential duration remains longer while CV and ERP returned to normal values 60 days after ablation. At 4 mm from the lesion, ERP, and APD were significantly elevated at several intermediate time points with respect to SHAM. At distances >4 mm ERP values showed transient changes while APD was not affected by the ablation procedure. At distances of 4 mm and >4 mm from the lesion, CV values demonstrated transient changes following ablation.

Energy delivery is associated with rapid and significant changes in electrophysiological parameters. Previous studies in multiple species have demonstrated significant electrophysiological effects of ablation beyond the border zone of the acute lesion.[12,13,17] However, few previous animal studies have reported electrophysiological changes >30 days post-operatively. We are not aware of any studies that have reported acute and chronic effects of transmural ablation in a survival ablation model. Specific electrophysiological parameters, including ERP and APD, have been shown to decrease with ablation both within and beyond the lesion. Wu *et al.*[12] performed optical voltage mapping of perfused rabbit hearts during and immediately after energy application. They reported APD_{80} decreased significantly compared with baseline both at the border zone and beyond the border zone during ablation. After cessation of energy delivery, APD_{80} at the border zone remained decreased and APD outside the border zone recovered within a few minutes. Longer-term studies of transmural ablation are limited; however, electrophysiological changes after ablation are thought to be similar to findings after myocardial infarction.[18–20]

Many investigators have demonstrated that biochemical markers of injury after ablation are similar to those found after myocardial injury due to ischaemia.[18–20] This finding suggests at least some common mechanisms of cellular death occur for both types of injury. Infarct studies have demonstrated similar sub-acute and chronic changes in electrophysiological parameters compared with our data. Hamada *et al.*[21] reported monophasic action potentials recorded during acute ischaemia in dogs. Similar to findings during acute ablation, APD values have been shown to significantly decrease after 5 min of coronary arterial occlusion and resolved within 15 min after relief of ischaemia. Long-term analysis of electrophysiological parameters following infarction in animal models demonstrates significant lengthening of APD and ERP. Pouliopoulos *et al.*[22] measured ERP ~5 months after myocardial infarction. These data were significantly increased in the partially scarred and fully scarred areas compared with baseline. Other studies have determined ERP in dogs with sub-acute and chronic completed infarction and demonstrated ERP values were longer in the infarcted hearts compared with controls but were unchanged in the sub-acute compared with the chronic animals.[23] Thus, our data are consistent with the notion that electrophysiological changes after myocardial injury due to ischaemia follow a similar time course as those after ablation. Similar to our findings, studies in rabbits and dogs have demonstrated that acute changes in electrophysiological parameters are not maintained chronically.[13,22]

Conclusions

We have successfully developed a novel murine survival model of ventricular ablation. For the first time, we have described the dynamic electrophysiological changes in the intact murine heart, in sub-acute and chronic ablation lesions. We have shown that subxiphoid ablation results in reproducible, transmural lesions. The transmural lesions are associated with significant changes in ERP, CV, and APD both near and remote from the lesion site. Action potential duration and ERP parameters beyond the lesion border recover within 60 days after ablation. These observations are consistent with previous studies in larger animal models. A survival murine model of ablation provides a new tool to investigate the molecular mechanisms of electrophysiological changes following ablation.

Clinical implications

Radio frequency ablation is the mainstay of catheter-based ablation strategies for many cardiac arrhythmias. Despite ongoing improvements in technology, arrhythmia recurrence continues to be a major clinical problem especially in the treatment of complex arrhythmias, including AF and ventricular tachycardias. Clinical endpoints of ablation are based on predictors of long-term success including arrhythmia termination, failure to re-induce arrhythmias, and confirmation of bi-directional conduction block across linear lesions sets. These phenomena are in turn dependent on the electrophysiological effects of RF ablation. Arrhythmias with very low recurrence rates after RF ablation, such as typical right atrial flutter, are typically re-entrant or focal in aetiology, originating from a small well-defined area of myocardium. Arrhythmias with higher recurrence rates, such as ventricular tachycardia and AF, involve a more widespread area of myocardium. These arrhythmias are subject to electrophysiological effects of RF ablation, which occur remote from the ablation site. We have demonstrated in a

murine model of healed ablation lesions, APD, and ERP changes beyond the lesion border return to normal values within 60 days. The clinical effects of this phenomenon are two-fold: (i) an acute clinical success may not translate into long-term success; and (ii) critical areas of arrhythmogenesis remote from the initial areas of ablation may not be identified during the ablation procedure. This study suggests that dynamic changes in electrophysiological parameters take place following lesion delivery, which should be considered when performing complex cardiac ablation procedures.

Limitations

There are a few limitations of this study. First, the electrophysiological properties following lesion delivery were evaluated in isolated hearts. It is possible that electrophysiological parameters in the intact animal may differ. Second, this study was performed using mice. Using small animal models allows for a large number of animals to be followed for a longer periods of time. However, there are important limitations related to the distinct electrophysiology of small animals. Although mechanisms of impulse propagation are likely to be similar in large and small animals the ionic currents that contribute to re-polarization differ significantly. It is possible that the temporal electrophysiological changes that were reported may differ slightly in larger animals.

Conflict of interest: none declared.

Funding

This work was supported by grants from the National Institutes of Health National Heart Lung and Blood Institute (HL076751 to GEM, 1T32HL098129 to C.V.), the American Heart Association to (a Health Sciences Student Research Fellowship to J.M.L. and 0725898T to C.V.), Alpha Omega Alpha (a Carolyn L. Kuckein Student Research Fellowship to JML), and the New York Academy of Medicine (a Glorney-Raisbeck Fellowship to JML).

References

1. Reddy VY, Reynolds MR, Neuzil P, Richardson AW, Taborsky M, Jongnarangsin K *et al.* Prophylactic catheter ablation for the prevention of defibrillator therapy. *N Engl J Med* 2007;**357**:2657–65.
2. Stevenson WG. Ventricular scars and ventricular tachycardia. *Trans Am Clin Climatol Assoc* 2009;**120**:403–12.
3. Cano O, Hutchinson M, Lin D, Garcia F, Zado E, Bala R *et al.* Electroanatomic substrate and ablation outcome for suspected epicardial ventricular tachycardia in left ventricular nonischemic cardiomyopathy. *J Am Coll Cardiol* 2009;**54**: 799–808.
4. Tanner H, Hindricks G, Volkmer M, Furniss S, Kuhlkamp V, Lacroix D *et al.* Catheter ablation of recurrent scar-related ventricular tachycardia using electroanatomical mapping and irrigated ablation technology: results of the prospective multicenter euro-vt-study. *J Cardiovasc Electrophysiol* 2010;**21**:47–53.
5. Gonska BD, Brune S, Bethge KP, Kreuzer H. Radiofrequency catheter ablation in recurrent ventricular tachycardia. *Eur Heart J* 1991;**12**:1257–65.
6. Marchlinski FE, Callans DJ, Gottlieb CD, Zado E. Linear ablation lesions for control of unmappable ventricular tachycardia in patients with ischemic and non-ischemic cardiomyopathy. *Circulation* 2000;**101**:1288–96.
7. Reddy VY, Neuzil P, Taborsky M, Ruskin JN. Short-term results of substrate mapping and radiofrequency ablation of ischemic ventricular tachycardia using a saline-irrigated catheter. *J Am Coll Cardiol* 2003;**41**:2228–36.
8. Soejima K, Suzuki M, Maisel WH, Brunckhorst CB, Delacretaz E, Blier L *et al.* Catheter ablation in patients with multiple and unstable ventricular tachycardias after myocardial infarction: short ablation lines guided by reentry circuit isthmuses and sinus rhythm mapping. *Circulation* 2001;**104**:664–9.
9. Forleo GB, Tondo C. Atrial fibrillation: cure or treat? *Ther Adv Cardiovasc Dis* 2009; **3**:187–96.
10. Wright M, Haissaguerre M, Knecht S, Matsuo S, O'Neill MD, Nault I *et al.* State of the art: catheter ablation of atrial fibrillation. *J Cardiovasc Electrophysiol* 2008;**19**: 583–92.
11. Ouyang F, Ernst S, Chun J, Bansch D, Li Y, Schaumann A *et al.* Electrophysiological findings during ablation of persistent atrial fibrillation with electroanatomic mapping and double lasso catheter technique. *Circulation* 2005;**112**:3038–48.
12. Wu CC, Fasciano RW II, Calkins H, Tung L. Sequential change in action potential of rabbit epicardium during and following radiofrequency ablation. *J Cardiovasc Electrophysiol* 1999;**10**:1252–61.
13. Wood MA, Fuller IA. Acute and chronic electrophysiologic changes surrounding radiofrequency lesions. *J Cardiovasc Electrophysiol* 2002;**13**:56–61.
14. Morley GE, Danik SB, Bernstein S, Sun Y, Rosner G, Gutstein DE *et al.* Reduced intercellular coupling leads to paradoxical propagation across the purkinje-ventricular junction and aberrant myocardial activation. *Proc Natl Acad Sci USA* 2005;**102**:4126–9.
15. Fedorov VV, Lozinsky IT, Sosunov EA, Anyukhovsky EP, Rosen MR, Balke CW *et al.* Application of blebbistatin as an excitation–contraction uncoupler for electrophysiologic study of rat and rabbit hearts. *Heart Rhythm* 2007;**4**:619–26.
16. Morley GE, Vaidya D, Samie FH, Lo CW, Delmar M, Jalife J. Characterization of conduction in the ventricles of normal and heterozygous connexin43 knockout mice using optical mapping. *J Cardiovasc Electrophysiol* 1999;**10**:1361–75.
17. Becker R, Bauer A, Senges JC, Schreiner KD, Voss F, Kuebler W *et al.* Effect of radiofrequency ablation on atrial myocardium. *Basic Res Cardiol* 2001;**96**:478–86.
18. Katritsis DG, Hossein-Nia M, Anastasakis A, Poloniecki J, Holt DW, Camm AJ *et al.* Myocardial injury induced by radiofrequency and low energy ablation: a quantitative study of ck isoforms, ck-mb, and troponin-t concentrations. *Pacing Clin Electrophysiol* 1998;**21**:1410–6.
19. Brueckmann M, Wolpert C, Bertsch T, Sueselbeck T, Liebetrau C, Kaden JJ *et al.* Markers of myocardial damage, tissue healing, and inflammation after radiofrequency catheter ablation of atrial tachyarrhythmias. *J Cardiovasc Electrophysiol* 2004;**15**:686–91.
20. Haegeli LM, Kotschet E, Byrne J, Adam DC, Lockwood EE, Leather RA *et al.* Cardiac injury after percutaneous catheter ablation for atrial fibrillation. *Europace* 2008;**10**:273–5.
21. Hamada K, Yamazaki J, Nagao T. Shortening of monophasic action potential duration during hyperkalemia and myocardial ischemia in anesthetized dogs. *Jpn J Pharmacol* 1998;**76**:149–54.
22. Pouliopoulos J, Thiagalingam A, Eipper VE, Campbell C, Ross DL, Kovoor P. Transmural mapping of myocardial refractoriness and endocardial dispersion of repolarization in an ovine model of chronic myocardial infarction. *Pacing Clin Electrophysiol* 2009;**32**:851–61.
23. Horvath G, Racker DK, Goldberger JJ, Johnson D, Jain S, Kadish AH. Electrophysiological and anatomic heterogeneity in evolving canine myocardial infarction. *Pacing Clin Electrophysiol* 2000;**23**:1068–79.